JLB

Article

Inhibition of NADPH oxidase activation by peptides mapping within the dehydrogenase region of Nox2-A "peptide walking" study

Iris Dahan, Shahar Molshanski-Mor, and Edgar Pick[1]

The Julius Friedrich Cohnheim Laboratory of Phagocyte Research, Department of Clinical Microbiology and Immunology, Sackler School of Medicine, Tel Aviv University, Tel Aviv, Israel

RECEIVED OCTOBER 8, 2011; REVISED NOVEMBER 22, 2011; ACCEPTED NOVEMBER 22, 2011. DOI: 10.1189/jlb.1011507

ABSTRACT

In this study, the "peptide walking" approach was applied to the DH region of Nox2 (residues 288–570) with the purpose of identifying domains of functional importance in the assembly and/or catalytic function of the NADPH oxidase complex of phagocytes. Ninety-one overlapping 15-mer peptides were synthesized to cover the full length of the Nox2 DH region, and these were tested for the ability to interfere with the activation of the oxidase in vitro in two semirecombinant cell-free systems. The first consisted of phagocyte membranes p47^{phox}, p67^{phox}, and Rac1 and an amphiphile; the second was p47^{phox}- and amphiphile-free and contained prenylated Rac1. We identified 10 clusters of inhibitory peptides with IC_{50} values of 10 μM, all of which were inhibitory, also in the absence of p47^{phox}. Based on the identification of residues shared by peptides in a particular cluster, we defined 10 functional domains in the Nox2 DH region. One domain corresponded to one FAD-binding subdomain, and four domains overlapped parts of three NADPH-binding subdomains. As expected, most inhibitory peptides acted only when added prior to the completion of oxidase assembly, but peptides associated with two NADPH-binding subdomains were also active after assembly. Kinetic analysis demonstrated that inhibition by peptides was not explained by competition for substrates (FAD, NADPH) but was of a more complex nature: noncompetitive with respect to FAD and uncompetitive with respect to NADPH. We conclude that oxidase-inhibitory peptides, in five out of 10 clusters identified, act by interfering with FAD- and NADPH-related redox reactions. ***J. Leukoc. Biol.*** **91: 501–515; 2012.**

Introduction

ROS represent central cytotoxic mediators in the destruction of pathogenic microorganisms by phagocytes (reviewed in ref. [1]). All ROS originate in the primordial oxygen radical, the $O_2^{\cdot -}$, generated by the NADPH-derived one-electron reduction of molecular oxygen. This reaction is catalyzed by a membrane-bound, 91-kDa flavoprotein known as gp91^{phox} (or Nox2), which is associated with a second membranal protein of 22 kDa (p22^{phox}) to form the flavocytochrome b_{558} heterodimer. Nox2 is 570 residues long and comprises six transmembrane α-helices linked by three outside-facing loops (A, C, and E), two cytosol-facing loops (B and D), and a long cytosolic segment, extending from residue 288 to 570. Nox2 is home to all redox stations supporting the flow of electrons from NADPH to oxygen, namely a NADPH-binding site and noncovalently bound FAD, present in the cytosolic part, and two nonidentical hemes, bound to histidine pairs present in the third and fifth membrane helices (reviewed in ref. [2]).

In the resting phagocyte, no electron flow occurs along the redox centers on Nox2. Its activation and the consequent production of $O_2^{\cdot -}$ require the stimulation of membrane receptors by the microorganisms to be phagocytosed or by soluble stimuli mimicking the physiological process [3], followed by a signal transduction cascade. The initiation of the electron flow is thought to be mediated by a conformational change in Nox2, which is the result of its interaction with one or more regulatory proteins present in the cytosol, in the resting cell, which translocate to the membrane upon phagocyte stimulation. The regulatory cytosolic components are p47^{phox}, p67^{phox}, p40^{phox}, and the small GTPase Rac (1 or 2). They translocate to the membrane environment of Nox2 to generate the activated $O_2^{\cdot -}$-producing NADPH oxidase complex (briefly, oxidase), a process known as oxidase assembly (reviewed in ref. [4]). Under physiological conditions in the intact cell, p47^{phox}, p67^{phox}, and Rac are all required for the induction of $O_2^{\cdot -}$

Abbreviations: AD=activation domain, AEBSF=4-(2-aminoethyl)benzenesulfonyl fluoride hydrochloride, CGD=chronic granulomatous disease, DH=dehydrogenase, K_m=Michaelis constant, LiDS=lithium dodecyl sulfate, $O_2^{\cdot -}$=superoxide anion, pI=isoelectric point, PRR=proline-rich region, ROS=reactive oxygen species, SH3=src 3 homology, TPR=tetratricopeptide repeats, V_{max}=maximum velocity

1. Correspondence: Department of Clinical Microbiology and Immunology, Sackler School of Medicine, Tel Aviv University, Tel Aviv 69978, Israel. E-mail: epick@post.tau.ac.il

production, whereas the role of p40^{phox} is less well-established. The consensus opinion is that p47^{phox}, p67^{phox}, and Rac establish direct molecular contacts with Nox2, but it is not clear whether interactions with all components are required for Nox2 activation. Indeed, a "monotheistic" model, in which p67^{phox} is seen as the paramount component responsible for the causation of a conformational remodeling of Nox2, was proposed [5, 6]. Consequently, considerable emphasis was placed on the identification of the region in p67^{phox}, essential for the productive interaction with Nox2, resulting in the proposal that such an AD comprises residues 199–210 [7] or a wider region, extending from residues 187 to 210 [8].

The encounter of Nox2 with one or more cytosolic components is preceded by preliminary interactions among cytosolic components. The two principal interactions are between a PRR at the C-terminus of p47^{phox} and the C-terminal SH3 domain of p67^{phox} and between the Switch 1 region of Rac and the TPR domain of p67^{phox}. In the monotheistic model, these are meant to facilitate the translocation to the membrane and/or specific binding of p67^{phox} to Nox2. Finally, p47^{phox} is involved in two more interactions: in the first, the tandem SH3 domains of p47^{phox} bind to a PRR in p22^{phox}; in the second, the phox homology region of p47^{phox} binds to specific membrane phosphoinositides. Both contacts bring p47^{phox} to the proximity of Nox2 and promote the binding of p47^{phox} and secondarily, that of p67^{phox} to Nox2.

The cytosolic segment of Nox2 is also known as the DH region by virtue of the fact that it contains the NADPH-binding site and noncovalently bound FAD [9–11]. These serve as the proximal redox stations, normally delivering the NADPH-derived two electrons to the hemes present in the membrane-associated segment, but under artificial conditions, electron flow can be diverted from reduced FAD to nonphysiological acceptors [12]. From an evolutionary perspective, the DH region of Nox2 is homologous to ferredoxin-NADP$^+$ reductase, a prokaryotic protein comprising NADPH- and FAD-binding domains [13]. The NADPH- and FAD-binding domains in the DH segment of Nox2 are noncontiguous when illustrated in the linear sequence of the protein, and the precise limits of the subdomains show some variation from author to author (reviewed in refs. [14–16]). In this study, we have adopted the limits, as described by Davis et al. [15]. Thus, the isoalloxazine and ribityl chain subdomains of the FAD-binding domain were mapped to residues 335–345 and 350–360, respectively, and the pyrophosphate, ribose, adenine, and nicotinamide subdomains of the NADPH-binding domain were mapped to residues 406–416, 442–447, 504–508, and 535–539, respectively.

The DH region was also found to be home to multiple binding sites for p47^{phox} (reviewed in ref. [2]) and more recently, to Rac [17], but so far, there is no published evidence about binding sites for p67^{phox}, although the existence of such sites is an integral part of all models of oxidase assembly proposed so far. There is also no information about the presence in the DH region of Nox2 of binding sites for p40^{phox}.

Synthetic peptides corresponding to specific regions in oxidase components represent a powerful tool for the detection and characterization of functional domains in these components. From a methodological perspective, two main approaches were used. In the first, termed peptide-phage display analysis, a peptide bacteriophage library is incubated with an immobilized oxidase component, and the bound phage is eluted, amplified, and analyzed for the presence of sequences corresponding to those present in other oxidase components. This technique was used successfully for the identification of Nox2 sequences involved in binding of p47^{phox} [18]. The second approach makes use of the availability of the cell-free oxidase activation system, in which a mixture of membrane (or purified flavocytochrome b_{558}) and recombinant cytosolic components (p47^{phox}, p67^{phox}, and Rac) is generating $O_2{\cdot}^-$ in the presence of an anionic amphiphile serving as activator and NADPH (reviewed in refs. [19, 20]). In a variation of the canonical cell-free system, activation requires the participation of p67^{phox} and prenylated Rac only and occurs in the absence of an anionic amphiphile activator and of p47^{phox}. This second system, known as amphiphile-independent, is especially useful when emphasis is to be placed on activation of Nox2 in the absence of p47^{phox}.

The cell-free system was used extensively for assessing the inhibitory effect of peptides on oxidase activation, an approach that yielded a vast amount of information about domains in the various components involved in protein—protein interactions leading to oxidase assembly (reviewed in refs. [21, 22]). Our group has introduced a methodological approach to study the effect of peptides on oxidase activation in vitro, known as "peptide walking" [23]. This consists of first synthesizing peptides 15 residues in length "covering" the full or partial length of a protein (in this particular case, an oxidase component), each peptide overlapping its neighbors by 12 or 13 residues. The peptides are synthesized by the multipin method [24] allowing the production of a large number of peptides at a reasonable cost and are not purified individually. Their initial use is to screen for the peptides exhibiting an inhibitory effect on oxidase activation in the cell-free system, an ability that is normally expressed by clusters of vicinal peptides. This result is followed by its confirmation by using selected, purified peptides corresponding to the most inhibitory peptide(s) in each cluster, by subjecting the peptides to scrambling or inversion of sequence (retro-peptides), by quantification of inhibition by dose-response experiments, by establishing the temporal parameters of inhibition in relation to that of the process of oxidase assembly, by kinetic studies meant to confirm or negate the competitive nature of inhibition, and by variations in the cell-free assay (presence or absence of amphiphilic activator and presence or absence of a certain component, such as p47^{phox}).

Peptide walking was applied to the identification of functional domains in Rac1 [23], p47^{phox} [25], and p22^{phox} [26]. In this report, we describe its application to the DH region of Nox2. We have chosen to examine the effect of peptides covering the cytosolic segment of Nox2, extending from residue 288 to 570, based on the idea that this will lead to the identification or confirmation of sites involved in the binding of cytosolic components and/or of the ligands of the redox stations. We found the following; 1) oxidase activation was inhibited by peptides that associated in 10 clusters; 2) inhibition was apparent in amphiphile- and p47^{phox}-dependent and -independent

systems, and the pattern of the peptide clusters was markedly similar; 3) the major clusters of inhibitory peptides overlapped regions involved in the binding of FAD and NADPH—one cluster corresponded to one FAD-binding subdomain (out of two), and four clusters overlapped parts of three NADPH-binding subdomains (out of four); 4) unlike most oxidase inhibitory peptides described in the past, peptides belonging to two major clusters, corresponding to the NADPH-binding region, were also inhibitory when added after the assembly of the oxidase complex; 5) the peptides corresponding to FAD- and NADPH-binding regions did not exhibit the expected competitive kinetics regarding the respective substrates, indicating a more complex mechanism of action.

MATERIALS AND METHODS

Synthetic peptides

Ninety-one overlapping pentadecapeptides, spanning the C-terminal sequence of Nox2 from aa 288 to 570, were synthesized by the multipin synthesis method [24] by Mimotopes (Clayton, Victoria, Australia). Such sets of overlapping peptides, synthesized in accordance with specific requirements, are available commercially and are known as "PepSets". Peptides overlapped by 12 residues and were acetylated at the N-terminus and amidated at the C-terminus. The purity of the peptides ranged from 60% to 70% (based on random sampling) but was not known at the level of individual peptides. The freeze-dried peptides were dissolved in a mixture of 75 parts 1-methyl-2-pyrrolidone and 25 parts water (v/v) to a concentration of 1.5 mM. To assure solubilization, the peptide solutions were subjected to sonication, using five, 10-s pulses in a VCX 400 W ultrasonic processor equipped with a cup horn filled with an ice-water mixture (Sonics & Materials, Danbury, CT, USA). The peptide stock solutions were divided into 100 μl aliquots and kept frozen at −75°C. PepSets peptides were used exclusively for screening experiments. For work with individual peptides found active by initial screening, purified synthetic peptides were used. These peptides had a purity of ≥70%, and the particular purity and molecular size of individual peptides were determined by the manufacturer by reverse-phase high-pressure liquid chromatography and mass spectrometry, respectively, and were provided on the purchase of the peptides. For controlling the sequence specificity of oxidase inhibitory peptides, selected peptides were synthesized in scrambled form using the algorithm described before [26] or as peptides with reversed sequence (retro-peptides).

Chemicals

The following chemicals were obtained from Sigma-Aldrich (St. Louis, MO, USA): ferricytochrome *c* (from horse heart; 95% pure), NADPH (tetrasodium salt; 95% pure), FAD (disodium salt), thrombin (from human plasma; ≥2000 NIH units/mg protein), glutathione-agarose, AEBSF, and n-octyl β-D-glucopyranoside. LiDS was purchased from Merck KGaA (Darmstadt, Germany). Common laboratory chemicals at the highest purity available were purchased from Merck KGaA or Sigma-Aldrich.

Preparation of recombinant proteins

Full-length $p47^{phox}$ (1–390) and $p67^{phox}$ (1–526) were prepared in baculovirus-infected *Sf9* cells (as described in ref. [27]) and purified by preparative ion exchange chromatography on HiLoad SP Sepharose and Q Sepharose columns, respectively, as described before [28]. $p67^{phox}$ (1–212) and Rac1 mutant Q61L were expressed as GST fusion proteins in *Escherichia coli* BL21-Codon Plus competent cells (Stratagene, Agilent Technologies, Santa Clara, CA, USA) and purified by affinity chromatography on glutathione-agarose, followed by cleavage by thrombin in situ, as described before [29]. The proteolytic action of thrombin was stopped by the addition to the cleaved protein of 1 mM AEBSF. The chimeric protein [$p67^{phox}$ (1–212)-Rac1 Q61L (1–192)] was expressed in *E. coli* as a GST fusion protein and purified as described before [30]. AEBSF was reported to exert an inhibitory effect on cell-free oxidase activation with an IC_{50} of 0.87 mM [31]. The final concentrations of AEBSF in the cell-free oxidase activation assays, in which the inhibitory effect of peptides was assessed, were 100–400 times lower than the IC_{50}. Nevertheless, we performed control experiments in which AEBSF (10 μM) was added to the cell-free assays, and we found that it had no inhibitory effect on oxidase activation.

Determination of protein concentration and purity

The protein concentration of the recombinant proteins was measured by the method of Bradford [32], modified for use with 96-well microplates using Bio-Rad protein assay dye reagent concentrate (Bio-Rad Laboratories, Hercules, CA, USA) and bovine γ-globulin as a standard. The level of purity of the recombinant proteins was assessed by SDS-PAGE analysis, and the gels were stained with GelCode Blue stain reagent (Thermo Scientific, Rockford, IL, USA).

Enzymatic prenylation of Rac1 Q61L

Recombinant nonprenylated Rac1 was prenylated in vitro by recombinant mammalian geranylgeranyltransferase type I (a gift of Dr. Carolyn Weinbaum, Duke University, Durham, NC, USA), as described before [30].

Preparation of macrophage membrane vesicles

Phagocyte membranes were prepared from guinea pig macrophages obtained by injection of mineral oil into the peritoneal cavity as described [33]. The membranes were solubilized in 40 mM n-octyl β-D-glucopyranoside and then reconstituted into liposomes by dialysis against detergent-free buffer as described previously [34]. The specific cytochrome b_{558} heme content of membrane vesicles was measured by the difference spectrum of sodium dithionite-reduced minus oxidized samples [35].

Cell-free NADPH oxidase activation assays

Two variations of the cell-free oxidase assay were used. The canonical assay, known as the amphiphile- and $p47^{phox}$-dependent assay, involves the participation of phagocyte membranes (as a source of cytochrome b_{558}) $p47^{phox}$, $p67^{phox}$, and Rac in the GTP-bound form and an activating anionic amphiphile, such as arachidonate or SDS (or LiDS) [33, 36]. The second variation, known as the amphiphile- and $p47^{phox}$-independent assay, involves the participation of phagocyte membranes $p67^{phox}$ and prenylated Rac and does not require an amphiphilic activator [6]. A detailed description of both methodologies has been published [19].

The amphiphile-dependent assay

The assays were performed in 96-well flat-bottom polystyrene plates (Product Number 655101, Greiner Bio-One, Frickenhausen, Germany) at room temperature. Reaction mixtures contained membrane liposomes equivalent to 5 nM cytochrome b_{558} heme and $p47^{phox}$, $p67^{phox}$, and nonprenylated Rac1 Q61L, all at a concentration of 100 nM in oxidase assay buffer containing 10 μM FAD [37] supplemented with LiDS (130 μM) in a total volume of 200 μl. The plates were shaken for 1.5 min, and $O_2\cdot^-$ production was initiated by the addition of 10 μl 5 mM NADPH (resulting in a final concentration of 240 μM) and quantified by following the rate of cytochrome *c* reduction at 550 nm in a kinetic assay over a time period of 5 min [19] performed in a SpectraMax 340 microplate reader (Molecular Devices, Sunnyvale, CA, USA) using SoftMax Pro software. Blank values were represented by wells containing 200 μl assay buffer to which 10 μl of 5 mM NADPH was added simultaneously with its addition to the oxidase assay wells. Results were calculated from the linear portion of the absorbance at a 550-nm curve and expressed as the amount of $O_2\cdot^-$ produced/time unit/mol membrane cytochrome b_{558} heme (mol $O_2\cdot^-$/s/mol cytochrome b_{558} heme).

The amphiphile-independent assay

This assay was performed essentially as the amphiphile-dependent assay with the following differences: 1) no p47^{phox} was present; 2) Rac1 Q61L was prenylated; 3) no LiDS was added; 4) whereas membrane liposomes were present equivalent to 5 nM cytochrome b_{558} heme, p67^{phox} and prenylated Rac1 Q61L were added at a concentration of 300 nM; and 5) the incubation period was extended to 5 min with shaking. $O_2^{\cdot -}$ production was initiated by the addition of NADPH to a final concentration of 240 μM and quantified and expressed as described for the amphiphile-dependent assay.

Inhibition of NADPH oxidase activation by Nox2 peptides

The effect of overlapping Nox2 C-terminal pentadecapeptides on NADPH oxidase activation was tested in the two cell-free systems described above. Peptides from 1.5 mM stock solutions were diluted in assay buffer to a concentration of 100 μM, and amounts of 20 μl were added/well as the first component of the 200 μl reaction mixtures, resulting in a final concentration of peptide of 10 μM. To control wells, 20 μl assay buffer supplemented with 1-methyl-2-pyrrolidone was added to result in a final concentration of organic solvent identical to that found in the peptide-containing wells. This was followed by the addition of 150 μl of a mixture of p47^{phox}, p67^{phox}, and nonprenylated Rac1 Q61L to reach a final concentration of 100 nM each (in the amphiphile-dependent assay) or 160 μl of a mixture of p67^{phox} and prenylated Rac1 Q61L to reach a final concentration of 300 nM each (in the amphiphile-independent assay). The contents of the wells were incubated with mixing for 15 min at room temperature on an orbital 96-well plate shaker (Bellco, Vineland, NJ, USA) to allow the interaction between the peptide and one or more of the cytosolic components. Following this, 20 μl macrophage membrane liposomes, equivalent to a final concentration of cytochrome b_{558} heme of 5 nM and 10 μl assay buffer containing LiDS to achieve a final concentration of 130 μM, were added in the amphiphile-dependent assay. The 96-well plate was reincubated for 1.5 min at room temperature. In the amphiphile-independent assay, 20 μl macrophage membrane liposomes only were added, and the plate was reincubated for 5 min. In both cases, $O_2^{\cdot -}$ production was initiated by the addition of 10 μl NADPH to reach a final concentration of 240 μM. The effect of a peptide on NADPH oxidase activation was expressed as percent inhibition of NADPH oxidase activation, which was calculated by considering $O_2^{\cdot -}$ production by control mixtures in the absence of peptide as 100%. Taking into account experimental variability and past experience with this methodology [23, 25, 26], we considered arbitrarily values above 10% inhibition of oxidase activation as being significant, but the main criterion for inhibition being considered meaningful was the grouping of the inhibitory peptides in clusters, separated by inactive peptides.

The effect of Nox2 peptides added after NADPH oxidase assembly

The effect of Nox2 peptides after completion of NADPH oxidase assembly was tested in the two types of cell-free assay. In the first (amphiphile-dependent), reaction components were added in the following order: 20 μl peptide (10 μM), followed by 180 μl of a reaction mixture consisting of membrane liposomes (equivalent to 5 nM cytochrome b_{558} heme) p47^{phox}, p67^{phox} (1–526), nonprenylated Rac1 Q61L (all at a concentration of 100 nM), and LiDS (130 μM), which were preincubated for 1.5 min before addition to the wells. In the second (amphiphile-independent), 180 μl of a reaction mixture consisting of membrane liposomes (equivalent to 5 nM cytochrome b_{558} heme) p67^{phox} (1–526) and prenylated Rac1 Q61L (all at a concentration of 300 nM), which were preincubated for 5 min in the absence of LiDS, was added to the wells containing 20 μl peptide (10 μM). In both situations, the reaction mixtures were incubated with the peptides for an additional 15 min, and $O_2^{\cdot -}$ production was initiated by the addition of 10 μl NADPH (to result in a final concentration of 240 μM).

Determination of IC_{50} of peptides

The potential of the peptides to inhibit superoxide generation was quantified by measuring the concentration of peptides that reduced $O_2^{\cdot -}$ production by 50% (IC_{50}). This was determined by performing peptide concentration versus inhibition of oxidase activation dose-response curves using several concentrations of peptides (1.25, 2.5, 5, 10, 20, and 40 μM) in the amphiphile-independent NADPH oxidase cell-free assay with p67^{phox} (1–526) and prenylated Rac1 Q61L. IC_{50} values were calculated by using a nonlinear regression equation fit of the data [sigmoidal dose-response (variable slope)], plotted using GraphPad Prism Version 4.03 (GraphPad Software, La Jolla, CA, USA).

Kinetic analysis of inhibition by peptides

The mechanism of inhibition of superoxide generation by Nox2 peptides with respect to the concentrations of NADPH and FAD was examined in an amphiphile-independent cell-free assay with p67^{phox} (1–526) and prenylated Rac1 Q61L by assessing the effect of varying the concentrations of NADPH or FAD on the inhibition of NADPH oxidase activation by selected peptides, present at two concentrations. Kinetic parameters were determined by the Michaelis-Menten equation using linear regression fitting of the data, calculated, and plotted in Lineweaver-Burk format using GraphPad Prism Version 4.03.

RESULTS

Rationale and methodological optimization of peptide walking through Nox2

Ninety-one ovelapping peptides, 15 residues long and with a three-residues offset covering the entire length of the cytosol-exposed segment of Nox2 (residues 288–570), were synthesized. In accordance to the recommendation of the developers of epitope mapping by overlapping peptides, the N- and C-terminal ends were capped by acetylation and amidation, respectively [38]. The full list of peptides is illustrated in **Fig. 1**. Peptide synthesis was limited to the cytosolic tail of Nox2, based on the reasoning that this is the region most likely to be involved in interactions with cytosolic components and on the fact that it also comprises the NADPH- and FAD-binding domains. This choice leaves out the cytosolic loop B, reported to participate in the binding of p47^{phox} [18, 39] and in intramolecular interactions with the DH region [40], and loop D, which was implicated in electron transport from FAD to hemes and oxygen [41]. On the other hand, arguments were also put forward for the Nox2 C-terminus harboring all of the binding sites for the cytosolic components [42]. The full length of the cytosolic part of Nox2 was subjected to peptide walking; no preference was given to regions predicted to be hydrophilic, as reported in an earlier study [39], based on an analysis of the membrane topology of flavocytochrome b_{558} [43].

The peptides were synthesized based on the amino acid sequence of human Nox2 [44]. This raises the question of the extent of sequence similarity between human Nox2 and guinea pig Nox2, which forms part of the cytochrome b_{558} heterodimer present in the macrophage membranes used in the cell-free assays for assessing inhibition of oxidase activation by Nox2 peptides. We were not able to find information about the sequence of guinea pig Nox2 in the literature [15, 45]. Davis et al. [15] reported a 90.7–92.4% identity among the sequences of human, bovine, porcine, and murine Nox2. However, if one focuses on the two FAD-binding and the four NADPH-binding subdomains (which are at the core of the present

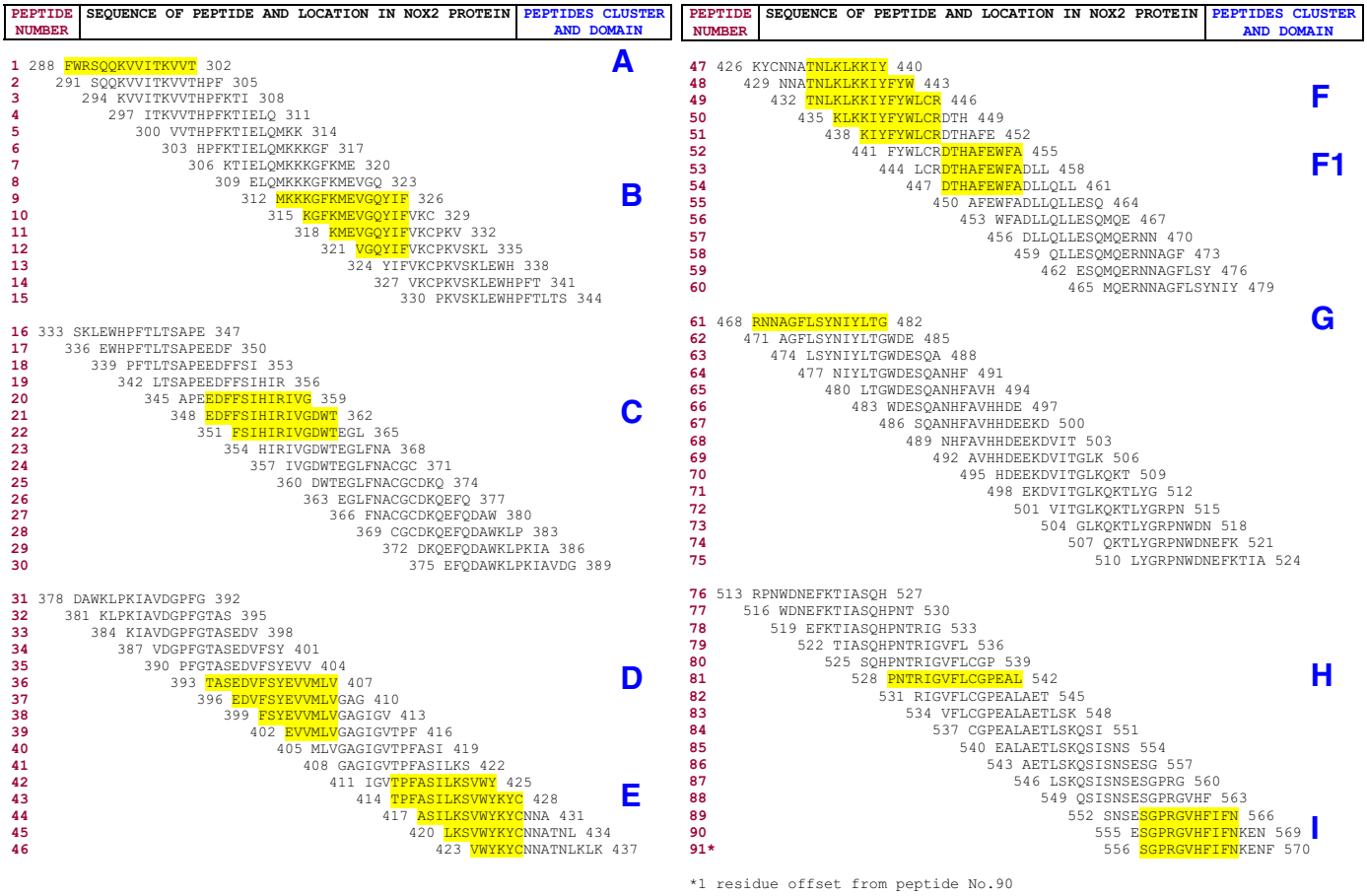

Figure 1. List of overlapping Nox2 DH region synthetic pentadecapeptides used in the inhibition of NADPH oxidase activation experiments. Residues in the peptides are in single-letter abbreviations. The numbers at the N- and C-terminus of each peptide indicate the location of the corresponding 15 residues in the amino acid sequence of Nox2. Residues highlighted in yellow represent residues shared by a cluster of peptides exhibiting NADPH oxidase inhibitory properties. The sequences corresponding to the peptides, in each cluster with the maximal inhibitory activity are considered as representing the closest approximation of the inhibitory "domains", although the precise limits of these domains remain, at this stage, hypothetical. The blue boldface, uppercase letters at the right of the list of peptides indicate the nomenclature of the clusters of inhibitory peptides (and corresponding sequence domains), as used throughout this article.

report), there is a 100% identity in the four species, increasing the likelihood that this is also the case with respect to guinea pig Nox2.

Because of the potential importance of hydrophobicity and charge in the inhibitory effect of peptides on oxidase activation, we have listed these two parameters for each of the peptides used in peptide walking, in a graphic form that allows relating these easily to the effect of the peptides on oxidase activation (**Fig. 2A** and **B**).

Inhibition of NADPH oxidase by Nox2 peptides was executed under conditions resulting in maximal sensitivity. This was assured by: 1) testing the peptides at a concentration (10 μM) 4000-fold higher than that of the flavocytochrome b_{558} present in the assays (5 nM heme, equaling 2.5 nM protein) and 2) having the cytosolic components in amphiphile-dependent and -independent, cell-free assays at concentrations located on the slope sections of dose-response curves (see ref. [19]), assuring a significant decrease in activity in a situation in which a Nox2 peptide would compete with the Nox2 protein for a cytosolic component or a redox site ligand.

The first group of peptide inhibition experiments was performed in the canonical amphiphile- and p47^{phox}-dependent system with full-length p67^{phox}. When these were repeated in the amphiphile- and p47^{phox}-independent system, we found an identical pattern of clustering for the inhibitory peptides with minor changes in the intensity of inhibition, mostly in the upward direction. This suggested that the assay methodology chosen reveals events principally or exclusively in the oxidase assembly process involving Nox2 and the cytosolic components p67^{phox} and Rac. Consequently, most of further work (peptide dose responses, sequence specificity of peptides, and kinetic analyses) was executed in the amphiphile- and p47^{phox}-independent system. This might appear as less physiological, because of the absence of p47^{phox}, but this is amply compensated by the use of a physiological form of Rac (prenylated) and by the emphasis on the Nox2–p67^{phox} interaction, which is considered as the central event in oxidase activation.

A further methodological issue was the order of adding the peptides in relation to the oxidase components to the cell-free

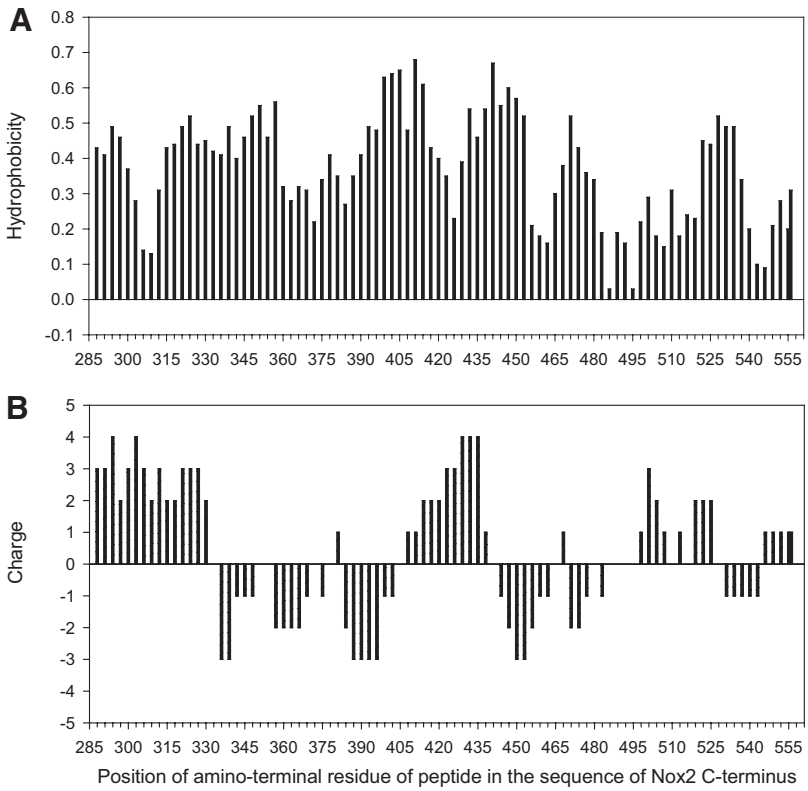

Figure 2. Hydrophobicity (A) and charge (B) plots of Nox2 DH region peptides. The hydrophobicity index of each peptide was calculated as the sum of indexes of individual amino acids composing the peptide (as described in ref. [46]). The net charge of each peptide was calculated as the sum of positive charges contributed by histidine, arginine, and lysine and the negative charges contributed by aspartate and glutamate.

assay. In all situations, the Nox2 peptides were preincubated with the cytosolic components for 15 min to offer an advantage to the Nox2 peptides over the Nox2 protein, represented by the membrane liposomes. Preliminary exploration of shorter and longer times of incubation did not yield results that were significantly different from the 15-min interval (incubation for 5 min was used in peptide walking applied to $p22^{phox}$ [26]). To gain more information about the mechanism of inhibition by peptides, we also designed an assay in which oxidase assembly preceded the addition of peptides.

Some Nox2 peptides, grouped in well-defined clusters, inhibit oxidase activation in amphiphile-dependent and -independent systems

As apparent in **Fig. 3A**, approximately one-quarter of the 91 overlapping Nox2 peptides exhibited significant inhibitory ability in the aphiphile-dependent assay with full-length $p67^{phox}$ when present at a concentration of 10 μM. One-half of the peptides inhibited oxidase activation at a level equal to or exceeding 40%, and some inhibited oxidase activation 80–90%. As expected from overlapping peptides and as found in similarly designed studies performed with Rac1, $p47^{phox}$, and $p22^{phox}$ [23, 25, 26], the inhibitory property was shared by groups of neighboring peptides, defined as clusters. As seen in Fig. 3A, we found four major clusters (B, C, E, and F), characterized by the intensity of inhibition and the number of strongly inhibitory peptides present in the cluster, and two minor clusters (D and F1). Three individual peptides were also found to be inhibitory (peptides 1, 61, and 81, based on numbering of peptides as appear in Fig. 1), and these were labeled A, G, and H, following the cluster nomenclature.

The peptides were next tested in the amphiphile- and $p47^{phox}$-free assay with full-length $p67^{phox}$. As seen in Fig. 3B, a pattern of inhibition and clustering essentially identical to that seen in Fig. 3A was found. Small differences were associated with peptides 61 and 81, now appearing as members of minor clusters (G and H), and with the emergence of an additional cluster (I) for the existence of which there was a hint in the results shown in Fig. 3A.

This section of the work was completed by examining whether replacing full-length $p67^{phox}$ with $p67^{phox}$ truncated at residue 212 will influence the pattern of inhibition by Nox2 peptides in the amphiphile- and $p47^{phox}$-free assay. Truncation of $p67^{phox}$ at residue 212 conserves the TPR and ADs but leaves out the PRR and both SH3 domains. We found that C-terminal truncation of $p67^{phox}$ does not cause a major change in the peptide inhibition pattern in comparison with that found in the parallel assay with full-length $p67^{phox}$ (Fig. 3C). The only differences are of a quantitative nature and are expressed in a reduction in the intensity of inhibition by peptides in most clusters, with the exception of clusters E and F, and in the absence of cluster G.

In a more limited number of experiments, we also examined the effect of Nox2 peptides in a cell-free oxidase activation system, in which the individual components $p67^{phox}$ (1–212) and Rac1 Q61L were replaced by the recombinant chimeric construct [$p67^{phox}$ (1–212)-Rac1 Q61L (1–192)]. This chimera was shown to be an effective oxidase activator

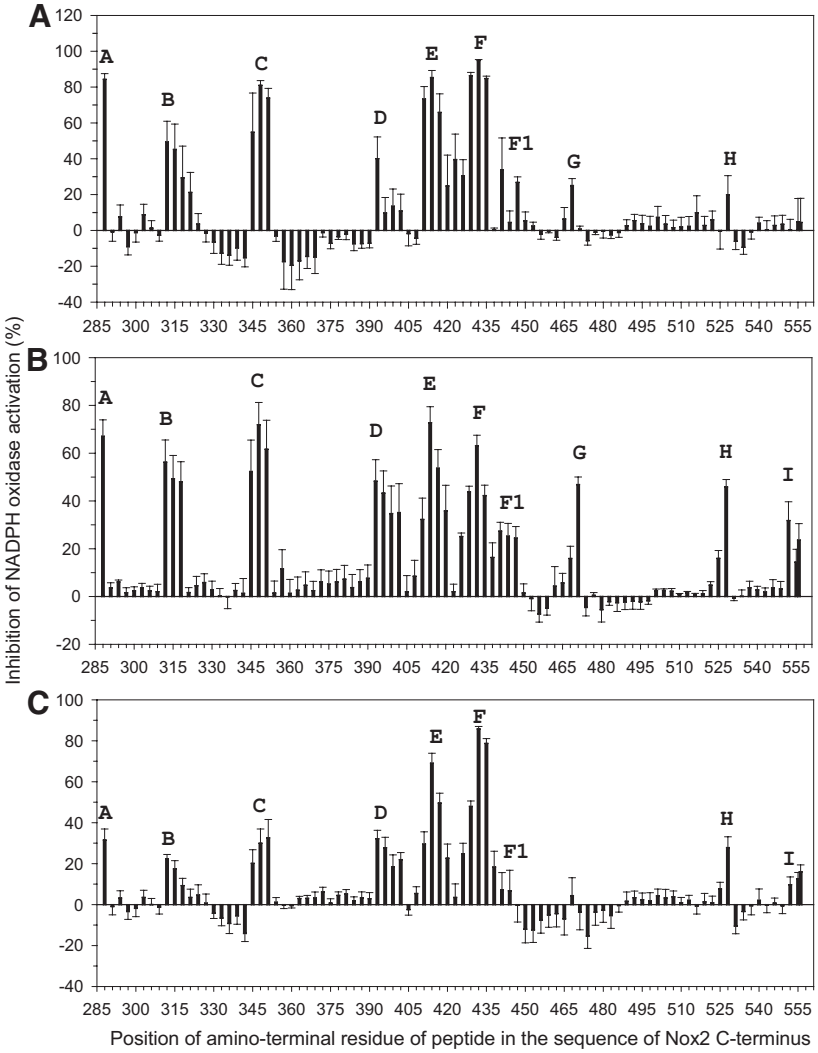

Figure 3. Inhibition of NADPH oxidase activation by Nox2 DH region peptides. (A) Inhibition in an amphiphile-dependent, cell-free system. Peptides, at a concentration of 10 μM, were tested for the ability to inhibit $O_2^{\cdot -}$ production in a LiDS-activated, cell-free system, consisting of solubilized macrophage membrane liposomes (equivalent to 5 nM cytochrome b_{558} heme) and recombinant p47^{phox} and p67^{phox} (1–526) and nonprenylated Rac1 Q61L, all at a concentration of 100 nM. The peptides were preincubated with the cytosolic components for 15 min before the addition of the membrane. LiDS was then added at a concentration of 130 μM, and following incubation for further 1.5 min, $O_2^{\cdot -}$ production was initiated by addition of 240 μM NADPH. (B) Inhibition in an amphiphile- and p47^{phox}-independent, cell-free system. Peptides were preincubated with p67^{phox} (1–526) and prenylated Rac1 Q61L, each at a concentration of 300 nM, for 15 min before the addition of the membrane. The mixtures were incubated for an additional 5 min before the addition of 240 μM NADPH. (C) Effect of C-terminal truncation of p67^{phox} on NADPH oxidase activation inhibition, which was measured in an amphiphile- and p47^{phox}-independent system containing p67^{phox} (1–212) instead of p67^{phox} (1–526). All results represent means ± SEM of three experiments. Uppercase, boldface letters A–I (including F1) denote the inhibitory peptide clusters.

in nonprenylated (with amphiphile and p47^{phox}) and prenylated (in the absence of amphiphile and p47^{phox}) forms (ref. [30] and reviewed in ref. [47]). The peptide inhibition pattern in an amphiphile-independent, cell-free assay, in which the activator was prenylated [p67^{phox} (1–212)-Rac1 Q61L (1–192)] chimera, was identical to that obtained when oxidase activation was elicited by the nonfused components (results not shown).

It could be deduced from the results obtained so far that the vast majority of inhibitory peptides could be identified by all of the assay variations used. Some differences in detection were apparent with clusters F1, G, H, and I, which were located in the C-terminal one-half of the cytosolic part of Nox2. A comparison of the peptide inhibition pattern with the hydrophobicity map (Fig. 2A) suggests no relationship between the two properties as far as the major clusters are concerned; a possible connection might apply to clusters G and H consisting of hydrophobic peptides. An analysis of the relationship between peptide charge (Fig. 2B) and inhibitory ability reveals a possible relationship between the strong positive charge (+4) and the inhibitory potency of the three most inhibitory peptides in cluster F (peptides 48, 49, and 50; based on numbering of peptides as appear in Fig. 1) and a possible role for a positive charge in the inhibitory effect of peptides in clusters A, B, and I.

In the experiments described above, the peptides were present at a uniform concentration of 10 μM. To gain information about their relative inhibitory potency, we ran peptide dose-response experiments, in which selected peptides representing the various clusters (the most inhibitory peptide in the cluster) were tested at concentrations from 1.25 to 40 μM in the amphiphile-independent NADPH oxidase cell-free assay with p67^{phox} (1–526) and prenylated Rac1 Q61L. The results of these experiments are summarized in **Table 1**. IC_{50} values for all peptides ranged between 3.58 and 9.15 μM, a result indicating that the choice of 10 μM as the concentration used in the screening experiments was appropriate. When taking into account the fact that the PepSets peptides were not purified, the true IC_{50} values are probably lower. At a later stage of this investigation, IC_{50} values were determined for purified peptides and for the corresponding scrambled or retro-peptides.

TABLE 1. IC_{50} Values of Representative (Most Inhibitory) Nox2 Peptides

Peptide number[a]	Peptide (sequence and location in Nox2)	Cluster	IC_{50} (μM)
1	^{288}FWRSQQKVVITKVVT^{302}	A	3.58
9	^{312}MKKKGFKMEVGQYIF^{326}	B	4.08
21	^{348}EDFFSIHIRIVGDWT^{362}	C	6.08
36	^{393}TASEDVFSYEVVMLV^{407}	D	3.92
43	^{414}TPFASILKSVWYKYC^{428}	E	6.09
49	^{432}TNLKLKKIYFYWLCR^{446}	F	5.18
61	^{468}RNNAGFLSYNIYLTG^{482}	G	6.54
81	^{528}PNTRIGVFLCGPEAL^{542}	H	9.15
89	^{552}SNSESGPRGVHFIFN^{566}	I	5.38

Selected Nox2 peptides, representing clusters A–I, derived from the PepSets peptide array used to screen for oxidase inhibition (Fig. 3), were tested for inhibition of oxidase activation in peptide dose-response experiments. The amphiphile- and $p47^{phox}$-independent, cell-free system was used with $p67^{phox}$ (1–526) and prenylated Rac1 Q61L, and IC_{50} values were calculated as described in Materials and Methods. Results are those of a representative experiment. [a]Based on numbering of peptides as appear in Fig. 1.

Two clusters of Nox2 peptides are capable of reversing oxidase assembly

On most occasions, when peptides were tested for an inhibitory effect on oxidase activation, they were found to act only when added before the assembly of an active complex (reviewed in refs. [21, 22]). We thus performed peptide walking experiments in which oxidase components were first mixed, resulting in assembly, and the PepSets peptides were added as the last component. Experiments were performed in the amphiphile-dependent system (**Fig. 4A**) and in the amphiphile- and $p47^{phox}$-independent

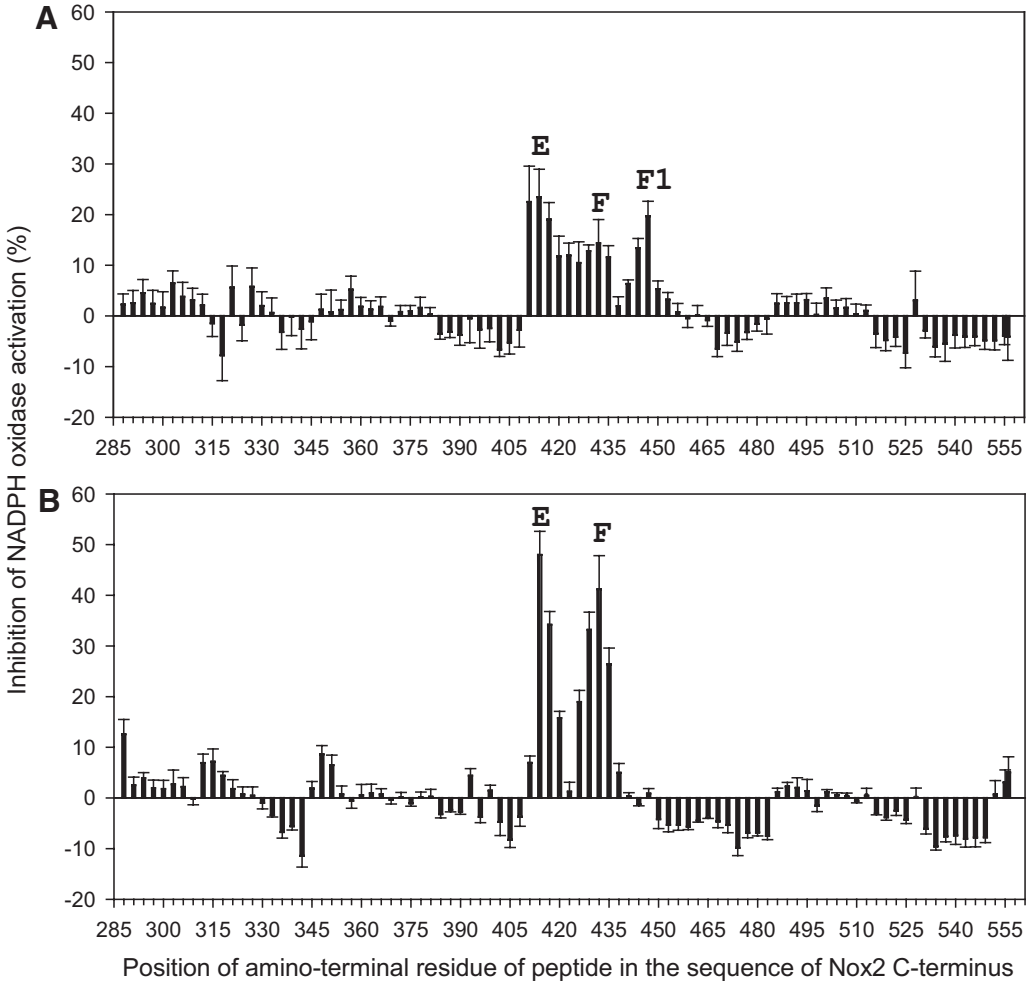

Figure 4. Some Nox2 peptides are capable of interfering with NADPH oxidase activation when added after the completion of amphiphile-dependent or -independent NADPH oxidase assembly. (A) A mixture consisting of membrane, $p47^{phox}$, $p67^{phox}$ (1–526), and nonprenylated Rac1 Q61L was preincubated with 130 μM LiDS for 1.5 min (resulting in oxidase assembly), and aliquots were added to wells of 96-well plates containing the individual Nox2 peptides. After 15 min incubation, NADPH was added to initiate $O_2\cdot^-$ production. (B) A mixture consisting of membrane, $p67^{phox}$ (1–526), and prenylated Rac1 Q61L was incubated for 5 min in the absence of amphiphile (resulting in oxidase assembly) and aliquots added to wells of 96-well plates containing the individual Nox2 peptides. After 15 min incubation, NADPH was added to initiate $O_2\cdot^-$ production. For methodological details, see Materials and Methods. Results illustrated in A and B represent means ± SEM of three experiments.

system (Fig. 4B). The results illustrated in these two figures should be compared with the parallel situations, in which peptides were added as the first components of the assay (Fig. 3A and B, respectively).

In both types of assay, peptides belonging to clusters E and F exhibited significant inhibitory action; some effect was also seen with cluster F1 peptides in the amphiphile-dependent assay (Fig. 4A). The degree of inhibition was less pronounced than in the assays in which peptides were added first. It is also apparent that the postassembly effect is more pronounced in the amphiphile- and $p47^{phox}$-independent assay.

These results could be interpreted as indicating that peptides in clusters E and F interfere with an event in the catalytic phase of $O_2^{\cdot -}$ production, involving the binding of NADPH or FAD (which is noncovalently bound to Nox2 [48]). We thus performed the above experiments in the presence of concentrations of FAD or NADPH, tenfold higher than those present in the standard reaction mixtures. This caused no change in the postactivation peptide inhibition pattern (results not shown).

Sequence specificity of oxidase inhibition by peptides

To ascertain that the dose-response studies performed with nonpurified peptides were accurate, we repeated these experiments with purified representative peptides belonging to clusters D, C, E, F, and G. The peptides selected were those that were the most effective in the clusters identified by the peptide walking experiments. We attempted to have scrambled peptides synthesized for each of the selected peptides. As a result of the fact that synthesis of a scrambled version of peptide 21 (cluster C) was repeatedly unsuccessful, we replaced this with a retro-peptide, as retro-peptides are frequently used as controls for sequence specificity (reviewed in ref. [49]). Dose-response experiments were successful for all peptides with the exception of purified peptide 36 (cluster D), which did not yield a sigmoid curve, required for calculation of IC_{50} values. The dose-response plots and IC_{50} values of native and scrambled peptides of clusters C, E, F, and G are shown in **Fig. 5**. It is apparent that the IC_{50} values of the native purified peptides are similar to those found with nonpurified PepSets peptides (Table 1). Scrambling of representative peptides belonging to clusters E, F, and G resulted in the reduction of inhibitory of potency, which was pronounced for clusters E and G (leading to an inability to determine IC_{50} values for the scrambled peptides), and moderate for cluster F (resulting in a close to twofold increase in IC_{50}). Unexpectedly, the retro-peptide corresponding to the peptide representing cluster C was as potent an inhibitor as the native peptide, as expressed in no significant change in IC_{50}.

Location of domains deduced from clusters of oxidase inhibitory peptides in the Nox2 cytosolic segment

Relying on the experience of previous peptide walking studies [23, 25, 26], we defined sequence domains for each cluster of inhibitory peptides. These domains represent the most likely

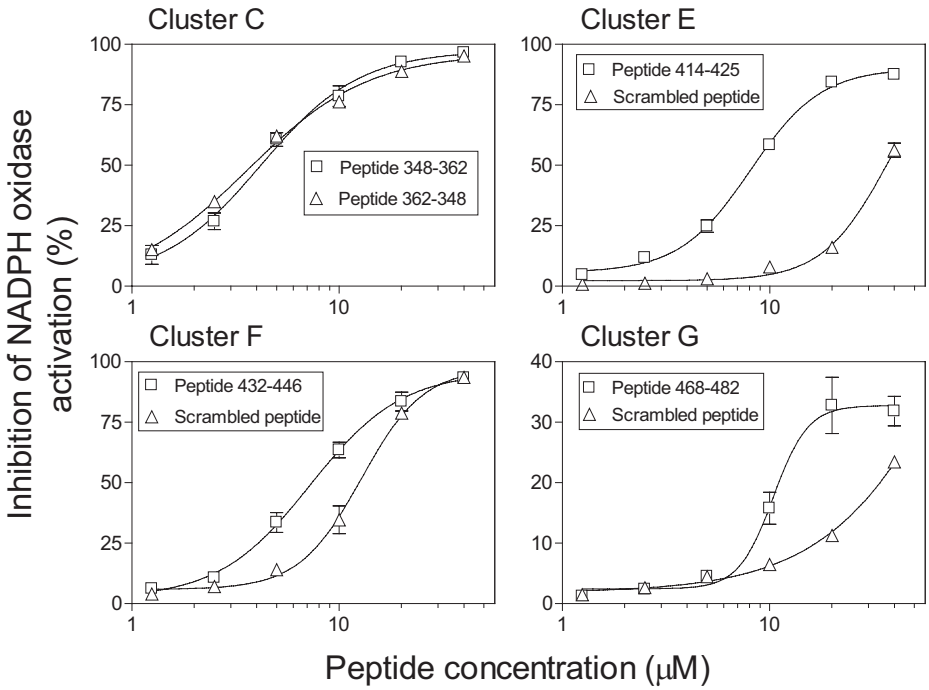

Figure 5. Dose-response curves of representative peptides belonging to clusters C, E, F, and G in comparison with the scrambled or retro-peptide versions. Selected, synthetic Nox2 peptides in the native and scrambled or retro-peptide forms (≥70% pure), representing clusters C, E, F, and G, were assayed for the ability to inhibit NADPH oxidase activation in an amphiphile- and $p47^{phox}$-free, cell-free system, consisting of membrane, $p67^{phox}$ (1–526), and prenylated Rac1 Q61L at concentrations ranging from 1.25 to 40 μM. Assay conditions were as detailed in the legend of Fig. 3B. Dose-response curves are depicted in the four panels. The table beneath the panels displays the IC_{50} values and (not determinable) indicates that the IC_{50} could not be determined because of the nonsigmoid nature of the curves representing the scrambled forms of the peptides representing clusters E and G. The results represent means ± SEM of three to six experiments.

Nox2 peptide (residues)	Cluster in Nox2 sequence	IC_{50} (μM)	
		Native	Scrambled[a] or retro-peptide[b]
348-362	C	4.19	3.62[b]
414-428	E	8.07	nd[a]
432-446	F	7.24	12.78[a]
468-482	G	10.41	nd[a]

Figure 6. Location of oxidase activation inhibitory domains in the linear representation of the Nox2 DH region in relation to the FAD- and NADPH-binding subdomains. (A) Nomenclature of inhibitory domains and the corresponding residues in the Nox2 sequence. (B) Location of the proposed inhibitory domains in the sequence of the Nox2 DH region is indicated by yellow highlighting and the blue outside border of the sequence segments and by the uppercase, blue boldface letters on the yellow background defining the domain above the highlighted segments. The two subdomains forming the FAD-binding region are indicated by the red font; the four subdomains, forming the NADPH-binding region, are indicated by the green font. The parts of the FAD and NADPH molecules, proposed to be engaged in binding to Nox2, are listed below the Nox2 sequence in red and green fonts, respectively.

A

Inhibitory domains	Putative limits of domains (residues)
A	288 - 302
B	312 - 326
C	348 - 362
D	393 - 407
E	414 - 428
F	432 - 446
F1	447 - 455
G	468 - 482
H	528 - 542
I	556 - 566

B

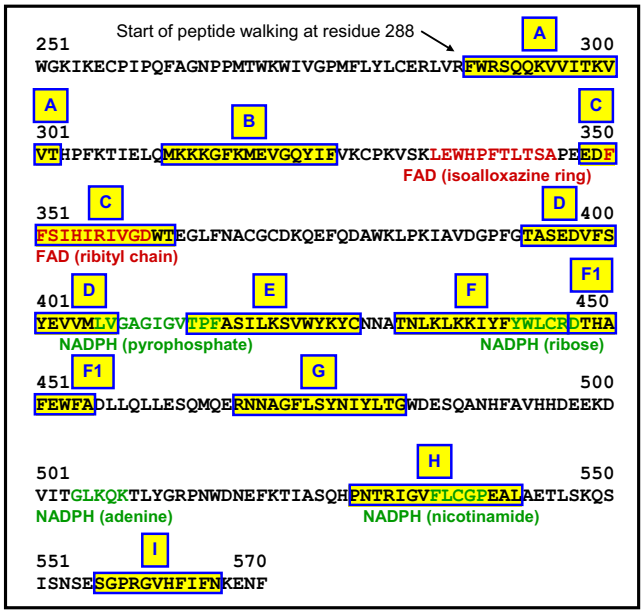

Nox2 sequence segment shared fully or in part by a cluster of oxidase inhibitory peptides. Defining the precise borders of such domains was beyond the purpose of this investigation and would have required N- and C-terminal truncations on numerous peptides. Thus, establishing the N- and C-terminal borders of the domains was principally based on the hypothesis that the peptide with the maximal inhibitory activity in each cluster is likely to comprise all or most of the domain. When a cluster did not contain a peptide with maximal activity, the domain was defined by the longest sequence shared by all peptides in the cluster (see clusters F1 and I). The way the clusters were defined is made obvious by the yellow highlighting of residues, shown in Fig. 1. The placement of the domains within the sequence of the DH region of Nox2 and their relationship to the known subdomains, of which the noncontiguous binding sites for FAD and NADPH are composed, are shown in the linear representation of the sequence (**Fig. 6**) and in the spatial illustration of the regions in the sequence contacting FAD and NADPH (**Fig. 7**).

It is apparent that there is a complete overlap between domain C and the ribityl chain-binding FAD subdomain. There is also significant, although lesser, overlap between domains D (C-terminus) and E (N-terminus) and the pyrophosphate-binding NADPH subdomain and considerable overlap between domain F (C-terminus) and the ribose-binding NADPH subdomain and between domain H and the nicotinamide-binding NADPH subdomain (in the latter case, the inhibitory domain comprises the full length of the NADPH-binding subdomain). It is of interest that a representative cluster C peptide (related to the ribityl chain-binding FAD subdomain) was equally active in the retro form, whereas peptides representing clusters E and F, belonging to NADPH-binding subdomains, exhibited high and moderate sequence specificity, respectively (Fig. 5).

No known, functionally important regions of Nox2 correspond to inhibitory domains A, B, and G. Domain F1 overlaps a region (residues 451–458), described previously as involved in the binding of $p47^{phox}$ [18]. Our results are not capable of providing a definite answer to this claim, but in our hands, inhibition of oxidase activation by cluster F1 peptides was also evident in the $p47^{phox}$- and amphiphile-independent system (Fig. 3B). In addition, recent evidence from our group indicates that Nox2 peptide 447–461, which overlaps domain F1, is involved in binding of $p67^{phox}$ (1–526) but not $p67^{phox}$ (1–212; unpublished results). As seen in Fig. 3B and C, peptides in cluster F1 are indeed preferentially interfering with oxidase activation by $p67^{phox}$ (1–526) and have a lesser effect on activation involving $p67^{phox}$ (1–212).

Domain I comprises residues 559–565, which correspond to yet another region reported to participate in the interaction of Nox2 with $p47^{phox}$. This proposal was based on mapping by peptide-phage display libraries [18] and on inhibition of oxidase activation by a Nox2 peptide containing these residues [51], but careful kinetic analysis did not support the proposed mechanism of the peptide competing with Nox2 for binding of $p47^{phox}$ [52].

Kinetic analysis of the mechanism of inhibition of oxidase activation by peptides comprising sequences belonging to FAD- and NADPH-binding subdomains

The fact that five out of 10 domains are connected to regions involved in the binding of FAD or NADPH suggested that inhibitory peptides could act by competing with the binding of the redox ligands to the DH region of Nox2. We approached this question by first performing a kinetic analysis of oxidase inhibition by a representative peptide of cluster C (comprising residues 348–362), which overlaps the full extent of the ribityl chain-binding FAD subdomain. The peptide was assayed in the $p47^{phox}$- and amphiphile-independent system with membranes preincubated with various concentrations of FAD (from 1 to 10 nM). To make possible the assessment of the effect of varying the concentration of FAD on inhibition, the assay buffer in these experiments did not contain FAD. The peptide

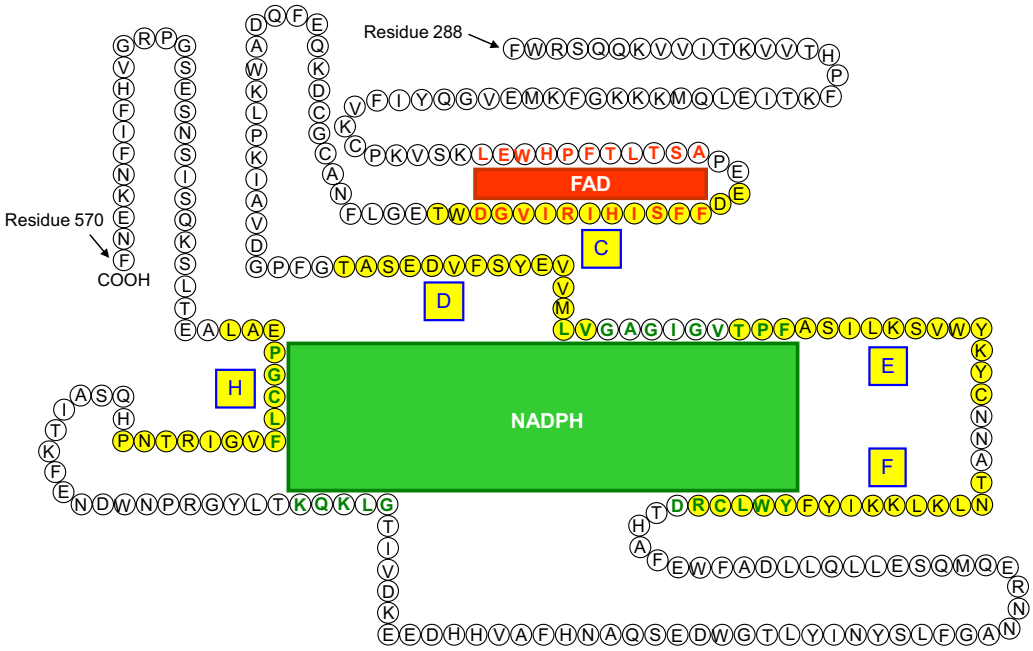

Figure 7. Schematic two-dimensional representation of the oxidase activation inhibitory domains in relation to the FAD- and NADPH-binding subdomains of the DH region of Nox2. The FAD-binding subdomains are shown in the red bold font and correspond to the isoalloxazine ring- and ribityl chain-binding subdomains (from the N- to the C-terminus). The NADPH-binding subdomains are shown in the green bold font and correspond, in succession, to the pyrophosphate, ribose, adenine, and nicotinamide-binding subdomains (from the N- to the C-terminus). The proposed inhibitory domains in the sequence of the Nox2 DH region are indicated by yellow highlighting of the residues forming the domains and by uppercase, blue boldface letters on the yellow background marking their nomenclature, as also appear in Fig. 6. Only domains that comprise parts of the FAD-binding (C) or NADPH-binding (D, E, F, and H) subdomains are shown. The representation of the DH region of Nox2 is purely schematic and was inspired by a figure in a publication by Clark et al. [50].

was assayed at two concentrations, encompassing the IC_{50} value, shown in Fig. 5. As apparent in **Fig. 8**, the cluster C peptide caused a two- and threefold decrease in the V_{max} value in proportion to increasing concentrations of peptide. However, there was no significant change in the K_m for FAD, and the Lineweaver-Burk plot was compatible with a noncompetitive inhibition mechanism, demonstrating that C cluster peptides do not act by competing with Nox2 for the binding of FAD.

We next performed a kinetic analysis of oxidase inhibition by representative peptides of clusters E (comprising residues 414–428) and F (comprising residues 432–446) in the $p47^{phox}$- and amphiphile-independent system, and the catalytic phase was initiated with NA-

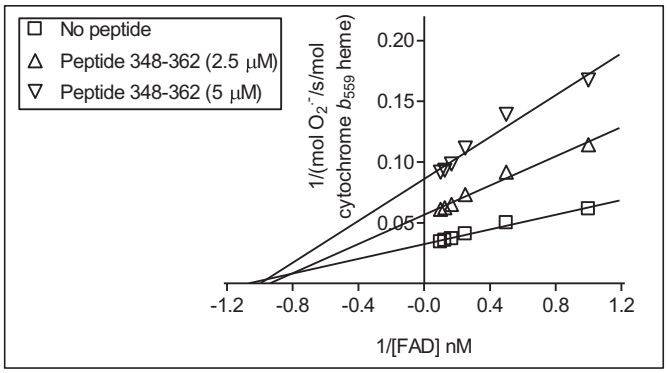

Peptide residues	Cluster in Nox2 sequence	Peptide concentration (μM)	V_{max} (mol $O_2^{\cdot-}$/s/mol cytochrome b_{558} heme)	K_m (nM FAD)
No peptide			33.90 ± 1.41	0.81 ± 0.04
348-362	C	2.5	17.67± 0.50	1.06
		5	11.60 ± 0.30	1.00

Figure 8. Kinetic analysis of inhibition of amphiphile-independent NADPH oxidase activation by a peptide from cluster C in relation to FAD concentration. Cluster C comprises oxidase inhibitory peptides sharing a sequence fully overlapping the ribityl chain subdomain of the FAD-binding region of Nox2. Peptide 348–362 (belonging to cluster C), at concentrations of 2.5 or 5 μM, was incubated with a mixture of $p67^{phox}$ (1–526) and prenylated Rac Q61L for 15 min. This was followed by the addition of membrane liposomes preincubated with FAD for 5 min (to result in final concentrations of FAD in the reaction of 1, 2, 4, 6, 8, and 10 nM) and incubation for 5 min. $O_2^{\cdot-}$ production was initiated by addition of NADPH (238 μM). Control mixtures were prepared under the same conditions but in the absence of peptides. The kinetic data are presented in double-reciprocal (Lineweaver-Burk) plots and represent means ± SEM of three experiments. The table beneath the plot displays V_{max} (NADPH oxidase activity) and K_m values (for FAD), derived by the kinetic analysis.

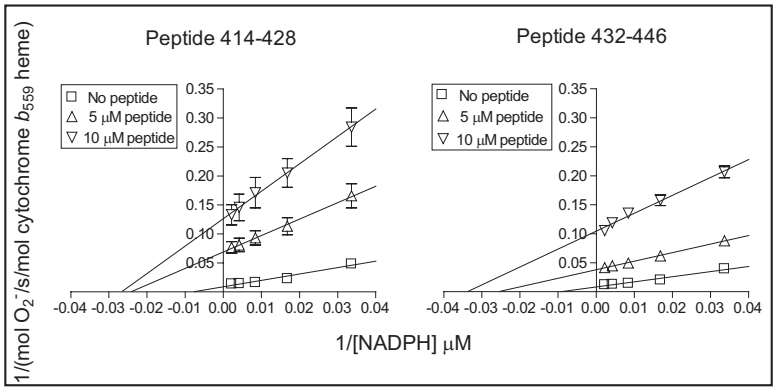

Figure 9. Kinetic analysis of inhibition of amphiphile-independent NADPH oxidase activation by peptides from clusters E and F in relation to NADPH concentration. Clusters E and F comprise oxidase inhibitory peptides sharing sequences partially overlapping the pyrophosphate and ribose subdomains of the NADPH-binding region of Nox2, respectively. Peptides 414–428 (cluster E) and 432–446 (cluster F), at concentrations of 5 and 10 μM, were incubated with p67^{phox} (1–526) and prenylated Rac1 Q61L for 15 min. This was followed by the addition of membrane liposomes, and after incubation for 5 min, $O_2^{\cdot -}$ production was initiated by addition of NADPH at concentrations varying from 28.37 to 454 μM (in twofold dilutions). Control mixtures were prepared under the same conditions but in the absence of peptides. The kinetic data are presented in double-reciprocal (Lineweaver-Burk) plots and represent means ± SEM of three experiments. The table beneath the plots displays V_{max} (NADPH oxidase activity) and K_m values (for NADPH) derived by the kinetic analysis.

Peptide residues	Cluster in Nox2 sequence	Peptide concentration (μM)	V_{max} (mol O_2^-/s/mol cytochrome b_{558} heme)	K_m (μM NADPH)
No peptide			114.00 ± 2.21	113.03 ± 8.14
414-428	E	5	14.50 ± 0.32	41.16
		10	7.91 ± 0.16	37.44
432-446	F	5	26.44 ± 0.67	39.59
		10	9.56 ± 0.29	29.59

DPH at concentrations varying form 28.37 to 454 μM in twofold dilutions. Peptide 414–428 partially overlaps the pyrophosphate binding and peptide 432–446, the ribose-binding NADPH subdomain. Both peptides were assayed at two concentrations encompassing the IC_{50} values shown in Fig. 5. As apparent in **Fig. 9**, both peptides caused a concentration-dependent decrease in the V_{max} value, in proportion to the increasing concentrations of the peptides. Unexpectedly, both peptides caused a three- to fourfold decrease in the K_m for NADPH in comparison with the value found for the uninhibited reaction. The Lineweaver-Burk plots for both peptides suggest that peptides in clusters E and F act via the relatively rare, uncompetitive inhibition mechanism and do not inhibit oxidase activation by simply competing with Nox2 for the binding of NADPH.

DISCUSSION

Our group is engaged in the systematic mapping of functional regions in all oxidase components by peptide walking. We have, so far, applied this approach to Rac1, p47^{phox}, and p22^{phox} [23, 25, 26], and the present report represents its application to the cytosol-exposed DH region of Nox2. Synthetic peptides, corresponding to restricted or extended regions of oxidase components, were used in functional assays, in which they served as inhibitors of oxidase activation (reviewed in refs. [21, 22]) and to a more limited extent, as partners in peptide–protein-binding assays (see general review, ref. [53] and its application to p47^{phox} [25] and p22^{phox} [26]).

Earlier work using synthetic peptides to explore Nox2 used a limited number of Nox2 peptides. These were chosen by one of the following approaches: screening by phage display library analysis for sites of interaction with p47^{phox} [18], testing a peptide used to generate an anti-Nox2 antibody found to block oxidase activation in the cell-free system [54], or testing selected Nox2 peptides corresponding to the most hydrophilic regions [39], based on Nox2 topology predictions [43]. To the best of our knowledge, ours is the first study using overlapping peptides covering the full length of the DH region of Nox2. All peptides were tested in a uniform way by strictly adhering to the methodological principles reiterated in a recent review [22]. A key issue was that the initial peptide walking was performed with all 91 peptides in the nonpurified form, but the quantitative and kinetic data were derived from the use of purified peptides.

The most studied, previously described oxidase inhibitory peptides, corresponding to the Nox2 DH region, include the following:

- Peptide 559–565 was described as corresponding to a Nox2 domain involved in the binding of p47^{phox} [18, 39, 51, 54, 55] and exhibiting sequence specificity [56]. It was claimed that it acted as a competitive inhibitor [55, 56], but kinetic analysis did not support this claim and suggested a more complex mechanism of action, such as binding to and altering the conformation of Nox2 [52].
- Peptide 452–464, first identified by mapping by peptide-phage display libraries, was found to be a rather weak oxidase inhibitor in vitro (IC_{50} of 230 μM) [18].
- Peptides 282–296, 304–321, and 434–455 were described as inhibitors in the canonical cell-free system [39]; among these, peptide 434–455 was found to prevent translocation

of p47^{phox} and p67^{phox} to the membrane in vitro. The IC_{50} values of these peptides and of peptide 559–565 were between 70 and 100 μM.

- Peptides 418–435 and 441–450, selected on the basis of the claim that they overlap NADPH-binding subdomains, were found to act as inhibitors in the canonical cell-free system with IC_{50} values between 10 and 60 μM [57]. One has to note that peptide 418–435 does not fit any of the accepted NADPH-binding subdomain sequences [14–16]. This peptide was reported to possess three unusual properties: it was inhibitory also when added after oxidase assembly; it was effective in a cell-free system activated in the absence of cytosolic components, as described in ref. [58]; and it exhibited uncompetitive kinetics with respect to NADPH.
- Peptide 491–504 was found to inhibit cell-free oxidase activation and the translocation of p47^{phox} and p67^{phox} in vitro. The peptide was studied because of the finding that a D500 to G mutation in a patient with the X91$^+$ form of CGD was associated with normal amounts of cytochrome b_{558} but impaired translocation of p47^{phox} and p67^{phox} [59].
- Peptide 419–430 was reported to inhibit cell-free oxidase activation and was proposed to be involved in the binding of Rac2 to Nox2 [17]. It is of interest that this peptide represents part of the sequence of peptide 418–435, to which different properties were attributed [57].

We have identified 10 domains in Nox2, the vast majority of which were represented by clusters of peptides with marked oxidase inhibitory activity in vitro (see Fig. 6). Domains A (288–302), B (312–326), and F + F1 (432–446+447–455) are likely to correspond to peptide sequences 282–296, 304–321, and 434–455, respectively, described in ref. [39]. Domain F + F1 also resembles the sequence of peptide 441–450 [57]. Domain E (414–428) corresponds to peptide 418–435, the minimum inhibitory sequence of which was found to be 420–425 [57], and to peptide 419–430 [17]; for the latter two peptides, contradictory functions in oxidase activation were proposed. Domain H (528–542) corresponds to peptide 526–549, described as a poor inhibitor [39]. Finally, domain I (556–566), which surprisingly, comprised peptides with rather modest inhibitory potency, closely resembles the sequence of the most investigated inhibitory Nox2 peptide 559–565 [18, 39, 51, 52, 54–56]. No equivalent to the inhibitory peptide 491–504 [59] was detected by us.

Our study revealed three previously unknown domains: C, D, and G (see Fig. 6). Domain C (348–362) is of special significance because of its perfect overlap with the ribityl chain-binding FAD subdomain (350–360). This is the first report of inhibition of oxidase activation by peptides belonging to a FAD-binding subdomain. It is of interest that this is limited to the sequence responsible for binding the ribityl chain and that peptides derived from the isoalloxazine-binding subdomain were not inhibitory. This is surprising in light of the fact that all mutations in the X91$^+$ form of CGD affecting FAD binding are located in the isoalloxazine-binding subdomain (ref. [60] and reviewed in refs. [61, 62]).

Oxidase activation inhibition by a representative domain C peptide was found to be independent of the amino acid sequence, as shown by the quasi-identical IC_{50} of a retro-isomer of the peptide. The most likely explanation for this finding is that the interaction between domain C peptide and its target involves hydrophobic and/or electrostatic forces. Indeed, Nox2 peptide 348–362 has a high hydrophobicity index (0.52, based on the scale described in ref. [46]), as a result of the presence of many hydrophobic residues. Lack of amino acid sequence specificity of oxidase activation inhibitory peptides was described in the past for C-terminal Rac1 peptides [63] and for peptides belonging to several domains in p22^{phox} [26]. In the latter case, scrambled and retro-peptides were interchangeable. Furthermore, oxidase inhibition by domain C peptides is not overcome by an excess of FAD and exhibits noncompetitive kinetics with respect to FAD. Thus, these peptides do not compete with the Nox2 protein for FAD binding and do not alter the affinity of FAD for Nox2 (no significant change in the K_m for FAD). The situation might be even more complex, as it was found that binding of FAD to Nox2 is affected (facilitated) by the oxidase-activating amphiphile and by the binding of cytosolic components [64]. Such noncompetitive (or mixed) kinetics were found unexpectedly to apply to the inhibition of oxidase activation by peptide 559–565 with respect to all cytosolic components [52].

Domain D peptides join those belonging to domains E, F, and H as representing a Nox2 sequence participating in the binding of NADPH. Thus, domains D and E contain residues involved in the binding of pyrophosphate, whereas domains F and H contain residues required for the binding of ribose and nicotinamide moieties of NADPH, respectively. The fact that domains F and F1 are contiguous, and their limits were decided on rather arbitrarily raises the possibility that domains F and F1 participate in binding of the ribose moiety and are de facto segments of a single larger domain. Oxidase inhibition by cluster E and F peptides is not reversed by an excess of NADPH and is characterized by the rather rare, uncompetitive kinetics with respect to NADPH. Such a kinetic pattern was described for oxidase inhibition by Nox2 peptide 418–435, which does not overlap an actual NADPH-binding subdomain but corresponds to the C-terminal part of domain E and the N-terminal part of domain F [57]. The conventional explanation for uncompetitive kinetics is that the inhibitor (peptide) binds to the enzyme-substrate complex (in our case, Nox2-NADPH) and causes a structural distortion, which renders it catalytically inactive without negatively affecting the affinity for the substrate, as shown by the paradoxical decrease in K_m for NADPH.

Peptides belonging to clusters E and F were also inhibitory when added after the completion of oxidase activation, which is a bidirectional process and is to a certain degree, reversible. We do not know which step, specifically, is reversed by E and F domain peptides, but the fact that these domains are involved in the binding of NADPH suggests that the peptides are likely to reverse a late, catalytic step involving interaction with NADPH. Interestingly, domain E and F peptides also shared with Nox2 peptide 418–435 the ability to act after the completion of oxidase assembly [57].

It is also significant that the two point mutations in the X91$^+$ form of CGD, shown to impair oxidase function by interfering with the binding of NADPH—P415 to H and C537 to R (ref. [60] and reviewed in refs. [61, 62])—are located in domains E and H, respectively. It should be made clear that kinetic analysis of oxidase inhibition by peptides belonging to domains C, E, and F was based on experiments performed with single representative peptides for each

domain in the belief that the results are applicable to all peptides in the clusters.

Our results do not permit to confirm or negate earlier reports linking particular Nox2 domains, defined by peptide-mediated inhibition of oxidase activation, to their role as binding sites for $p47^{phox}$ or Rac. As noted in Results, some of these proposals were not supported by our finding that inhibition by Nox2 peptides in the cell-free system in the presence and absence of $p47^{phox}$ revealed identical clusters. Our results do not permit us to offer an explanation for the mechanism of action of inhibitory peptides belonging to clusters A, B, G, and I. It is worth noting that peptides belonging to cluster G are hydrophobic, and those belonging to clusters A, B, and I are positively charged. The latter might interact by an electrostatic mechanism with anionic proteins, such as $p67^{phox}$ (1–526; pI=5.88) or the DH region of Nox2 itself (pI=6.82).

We believe that the very complex nature of the process of oxidase assembly and the fact that Nox2 interacts with all cytosolic components do not allow the drawing of direct conclusions on the identity of binding sites on Nox2 for these components from peptide inhibition of oxidase data only. The difficulties intrinsic to such an approach are illustrated by the findings that peptides belonging to the PRRs of $p47^{phox}$ and $p22^{phox}$ were found to bind $p67^{phox}$ and $p47^{phox}$, respectively, in peptide–protein-binding assays but were inactive as inhibitors of oxidase activation in vitro [25, 26]. The same caveat applies to the use of kinetic analysis; such analysis is most appropriate for a two-component enzyme: substrate situations and the fact that Nox2 interacts with three cytosolic components and two redox ligands, each containing more than one binding moiety, raise considerable difficulties of interpretation. The possibility that peptides may act by interfering with essential intramolecular interactions should be given serious consideration. A good example for such a situation is the recently described interaction between Nox4 and Nox2 loop B and the N-terminal one-half of their respective NADPH-binding domains, which was proposed to facilitate electron transport from the cytosolic to the membrane-localized redox centers [40]. Interference by DH region peptides with such an interaction seems an attractive hypothesis and might be associated with complex kinetics.

A more adequate interpretation of our findings will only be possible when the actual molecular structure of the DH region of Nox2 will become known, or at least, an adequate three-dimensional model will become available.

We conclude that inhibition of oxidase activation by Nox2 peptides is most useful in revealing sites involved in binding FAD and NADPH and thus, serving as redox centers. Only one of two FAD-binding and three out of four NADPH-binding subdomains were revealed by peptides; the isoalloxazine-binding site for FAD and the adenine-binding site for NADPH did not yield inhibitory peptides. The reason for the preference for subdomains binding smaller (ribityl, ribose, pyrophosphate) over those binding larger (isoalloxazine, adenine) polycyclic moieties is not clear.

Finally, peptide walking through the DH region of Nox2 also has an important practical aspect as a method for the design of peptides to be used as drugs for the therapy of the multiple disease states associated with the overproduction of Nox2-derived ROS. This issue has been the subject of two recent reviews [21, 22].

AUTHORSHIP

I.D. designed, performed, and analyzed the vast majority of the experiments and was involved in writing the paper. S.M-M. performed the kinetic experiments. E.P. contributed to the conceptual planning of the project, the design of the experiments, and writing the paper.

ACKNOWLEDGMENTS

This work was supported by Israel Science Foundation grant 49/09, the Roberts-Guthman Chair in Immunopharmacology, the Julius Friedrich Cohnheim-Minerva Center for Phagocyte Reserch, the Ela Kodesz Institute of Host Defense against Infectious Diseases, the Roberts Fund, and the Joseph and Shulamit Salomon Fund. The authors thank Thomas L. Leto (NIH) for providing baculoviruses carrying cDNA for $p47^{phox}$ and $p67^{phox}$ and for the GST-Rac1 expression plasmid, Frans Wientjes (University College, London, UK) for providing the GST-$p67^{phox}$ plasmid, and Patrick J. Casey and Carolyn Weinbaum (Duke University Medical Center) for providing recombinant geranylgeranyltransferase type I.

REFERENCES

1. Nauseef, W. M. (2007) How human neutrophils kill and degrade microbes: an integrated view. *Immunol. Rev.* **219,** 88–102.
2. Quinn, M. T., Gauss, K. A. (2004) Structure and regulation of the neutrophil respiratory burst oxidase: comparison with nonphagocyte oxidases. *J. Leukoc. Biol.* **76,** 760–781.
3. Pick, E., Keisari, Y. (1981) Superoxide anion and hydrogen peroxide production by chemically elicited peritoneal macrophages-induction by multiple non-phagocytic stimuli. *Cell. Immunol.* **59,** 301–318.
4. Groemping, Y., Rittinger, K. (2005) Activation and assembly of the NADPH oxidase: a structural perspective. *Biochem. J.* **386,** 401–416.
5. Kreck, M. L., Freeman, J. L., Abo, A., Lambeth, J. D. (1996) Membrane association of Rac is required for high activity of the respiratory burst oxidase. *Biochemistry* **35,** 15863–15682.
6. Gorzalczany, Y., Sigal, N., Itan, M., Lotan, O., Pick, E. (2000) Targeting of Rac1 to the phagocyte membrane is sufficient for the induction of NADPH oxidase assembly. *J. Biol. Chem.* **275,** 40073–40081.
7. Han, C-H., Freeman, J. L. R., Lee, T. H., Motalebi, S. A., Lambeth, J. D. (1998) Regulation of the neutrophil respiratory burst oxidase—identification of an activation domain in $p67^{phox}$. *J. Biol. Chem.* **273,** 16663–16668.
8. Grizot, S., Fieschi, F., Dagher, M-C., Pebay-Peyroula, E. (2001) The active N-terminal region of $p67^{phox}$: structure at 1.8 Å resolution and biochemical characterizations of the A128V mutant implicated in chronic granulomatous disease *J. Biol. Chem.* **276,** 21627–21631.
9. Rotrosen, D., Yeung, C. L., Leto, T. L., Malech, H. L., Kwong, C. H. (1992) Cytochrome b_{558}. The flavin-binding component of the phagocyte NADPH oxidase. *Science* **256,** 1459–1462.
10. Segal, A. W., West, I., Wientjes, F., Nugent, J. H. A., Chavan, A. J., Haley, B., Garcia, R. C., Rosen, H., Scarce, G. (1992) Cytochrome b-245 is a flavocytochrome containing FAD and the NADPH-binding site of the microbicidal oxidase of phagocytes. *Biochem. J.* **284,** 781–788.
11. Sumimoto, H., Sakamoto, N., Nozaki, M., Sakaki, Y., Takeshige, K., Minakami, S. (1992) Cytochrome b_{558}, a component of the phagocyte NADPH oxidase, is a flavoprotein. *Biochem. Biophys. Res. Commun.* **186,** 1368–1375.
12. Cross, A. R., Yarchover, J. L., Curnutte, J. L. (1994) The superoxide-generating system of human neutrophils possesses a novel diaphorase activity. *J. Biol. Chem.* **269,** 21448–21454.
13. Karplus, P. A., Daniels, M. J., Herriott, J. R., (1991) Atomic structure of ferredoxin-$NADP^+$ reductase: prototype for a structurally novel flavoenzyme family. *Science* **251,** 60–66.
14. Roos, D., De Boer, M., Kuribayashi, F., Meischl, C., Weening, R. S., Segal, A. W., Ahlin, A., Nemet, K., Hossle, J. P., Bernatowska-Matuszkiewicz, E., Middleton-Price, H. (1996) Mutations in the X-linked and autosomal recessive forms of chronic granulomatous disease. *Blood* **87,** 1663–1681.
15. Davis, A., Mascolo, P. L., Bunger, P. L., Sipes, K. M., Quinn, M. T. (1998) Cloning and sequencing of the bovine flavocytochrome *b* subunit proteins $gp91^{phox}$ and $p22^{phox}$: comparison with other flavocytochrome *b* sequences. *J. Leukoc. Biol.* **64,** 114–123.
16. Vignais, P. V. (2002) The superoxide-generating NADPH oxidase: structural aspects and activation mechanism. *Cell. Mol. Life. Sci.* **59,** 1428–1459.

17. Kao, Y-Y., Gianni, D., Bohl, B., Taylor, R. M., Bokoch, G. M. (2008) Identification of a conserved Rac binding site on NADPH oxidases supports a direct GTPase regulatory mechanism. *J. Biol. Chem.* **283,** 12736–12746.
18. DeLeo, F. R., Yu, L., Burritt, J. B., Loetterle, L. R., Bond, C. W., Jesaitis, A. J., Quinn, M. T. (1995) Mapping sites of interaction of p47^{phox} and flavocytochrome b with random-sequence peptide phage display libraries. *Proc. Natl. Acad. Sci. USA* **92,** 7110–7114.
19. Molshanski-Mor, S., Mizrahi, A., Ugolev, Y., Dahan, I., Berdichevsky, Y., Pick, E. (2007) Cell-free assays: The reductionist approach to the study of NADPH oxidase assembly, or "all you wanted to know about cell-free assays but did not dare to ask". In *Neutrophil Methods and Protocols* (M. T. Quinn, F. R. DeLeo and G. M. Bokoch, eds.), Humana Press, Totowa, NJ, 385–428.
20. Dagher, M-C., Pick, E. (2007) Opening the black box: lessons from cell-free systems on the phagocyte NADPH-oxidase. *Biochimie (Paris)* **89,** 1123–1132.
21. El-Benna, J., Dang, P. M-C., Perianin, A. (2010) Peptide-based inhibitors of the phagocyte NADPH oxidase. *Biochem. Pharmacol.* **80,** 778–785.
22. Dahan, I., Pick, E. (2011) Strategies for identifying synthetic peptides to act as inhibitors of NADPH oxidases, or "all that you did and did not want to know about Nox inhibitory peptides". *Cell. Mol. Life Sci.*, in press.
23. Joseph, G., Pick, E. (1995) "Peptide walking" is a novel method of mapping functional domains in proteins. Its application to the Rac1-dependent activation of NADPH oxidase. *J. Biol. Chem.* **270,** 29079–29082.
24. Valerio, R. M., Benstead, M., Bray, A. M., Campbell, R. A., Maeji, N. J. (1991) Synthesis of peptide analogues using the multipin peptide synthesis method. *Anal. Biochem.* **197,** 168–177.
25. Morozov, I., Lotan, O., Joseph, G., Gorzalczany, Y., Pick, E. (1998) Mapping of functional domains in p47^{phox} involved in the activation of NADPH oxidase by "peptide walking". *J. Biol. Chem.* **273,** 15435–15444.
26. Dahan, I., Issaeva, I., Sigal, N., Gorzalczany, Y., Pick, E. (2002) Mapping of functional domains in the p22^{phox} subunit of flavocytochrome b_{559} participating in the assembly of the NADPH oxidase complex by "peptide walking". *J. Biol. Chem.* **277,** 8421–8432.
27. Leto, T. L., Garrett, M. C., Fujii, H., Nunoi, H. (1991) Characterization of neutrophil NADPH oxidase factors p47^{phox} and p67^{phox} from recombinant baculovirus. *J. Biol. Chem.* **266,** 19812–19818.
28. Koshkin, V., Lotan, O., Pick, E. (1997) Electron transfer in the superoxide-generating NADPH oxidase complex reconstituted in vitro. *Biochim. Biophys. Acta* **1319,** 139–146.
29. Berdichevsky, Y., Mizrahi, A., Ugolev, Y., Molshanski-Mor, S., Pick, E. (2007) Tripartite chimeras comprising functional domains derived from the cytosolic NADPH oxidase components p47^{phox}, p67^{phox}, and Rac1 elicit activator-independent superoxide production by phagocyte membrane. *J. Biol. Chem.* **282,** 22122–22139.
30. Gorzalczany, Y., Alloul, N., Sigal, N., Weinbaum, C., Pick, E. (2002) A prenylated p67^{phox}-Rac1 chimera elicits NADPH-dependent superoxide production by phagocyte membranes in the absence of an activator and p47^{phox}. *J. Biol. Chem.* **277,** 18605–18610.
31. Diatchuk, V., Lotan, O., Koshkin, V., Wikstroem, P., Pick, E. (1997) Inhibition of NADPH oxidase activation by 4-(2-aminoethyl)-benzenesulfonyl fluoride and related compounds. *J. Biol. Chem.* **272,** 13292–13301.
32. Bradford, M. M. (1976) A rapid and sensitive method for the quantitation of microgram quantities of protein utilizing the principle of protein-dye binding. *Anal. Biochem.* **72,** 248–254.
33. Bromberg, Y., Pick, E. (1984) Unsaturated fatty acids stimulate NADPH-dependent superoxide production by cell-free system derived from macrophages. *Cell. Immunol.* **88,** 213–221.
34. Shpungin, S., Dotan, I., Abo, A., Pick, E. (1989) Activation of the superoxide forming NADPH oxidase in a cell-free system by sodium dodecyl sulfate. Absolute lipid dependence of the solubilized enzyme. *J. Biol. Chem.* **264,** 9195–9203.
35. Pick, E., Bromberg, Y., Shpungin, S., Gadba, R. (1987) Activation of the superoxide forming NADPH oxidase in a cell-free system by sodium dodecyl sulfate. Characterization of the membrane-associated component. *J. Biol. Chem.* **262,** 16476–16483.
36. Bromberg, Y., Pick, E. (1985) Activation of NADPH-dependent superoxide production in a cell-free system by sodium dodecyl sulfate. *J. Biol. Chem.* **260,** 13539–13545.
37. Toporik, A., Gorzalczany, Y., Hirschberg, M., Pick, E., Lotan, O. (1998) Mutational analysis of novel effector domains in Rac1 involved in the activation of nicotinamide adenine dinucleotide phosphate (reduced) oxidase. *Biochemistry* **37,** 7147–7156.
38. Rodda, S., Tribbick, G. (1996) Antibody-defined epitope mapping using the multipin method of peptide synthesis. *Methods* **9,** 573–481.
39. Park, M-Y., Imajoh-Ohmi, S., Nunoi, H., Kanegasaki, S. (1997) Synthetic peptides corresponding to various hydrophilic regions of the large subunit of cytochrome b_{558} inhibit superoxide generation in a cell-free system from neutrophils. *Biochem. Biophys. Res. Commun.* **234,** 531–536.
40. Jackson, H. M., Kawahara, T., Nisimoto, Y., Smith, S. M. E., Lambeth, J. D. (2010) Nox4 B-loop creates an interface between the transmembrane and dehydrogenase domains. *J. Biol. Chem.* **285,** 10281–10290.
41. Li, X. J., Grunwald, D., Mathieu, J., Morel, F., Stasia, M-J. (2005) Crucial role of two potential cytosolic regions of Nox2, ^{191}TSSTKTIRRS^{200} and ^{484}DESQANHFAVHHDEEKD^{500}, on NADPH oxidase activation. *J. Biol. Chem.* **280,** 14962–14973.
42. Von Löhneysen, K., Noack, D., Wood, M. R., Friedman, J. S., Knaus, U. G. (2010) Structural insights into Nox4 and Nox2: motifs involved in function and cellular localization. *Mol. Cell. Biol.* **30,** 961–975.
43. Imajoh-Ohmi, S., Tokita, K., Ochiai, H., Nakamura, M., Kanegasaki, S. (1992) Topology of cytochrome b_{558} in neutrophil membrane analyzed by anti-peptide antibodies and proteolysis. *J. Biol. Chem.* **267,** 180–184.
44. Royer-Pokora, B., Kunkel, L. M., Monaco, A. P., Goff, S. C., Newburger, P. E., Baehner, R. L., Cole, F. S., Curnutte, J. T., Orkin, S. H. (1986) Cloning the gene for an inherited human disorder—chronic granulomatous disease—on the basis of its chromosomal location. *Nature* **322,** 32–38.
45. Kawahara, T., Quinn, M. T., Lambeth, J. D. (2007) Molecular evolution of the reactive oxygen-generating NADPH oxidase (Nox/Duox) family of enzymes. *BMC Evolut. Biol.* **7,** 109.
46. Fauchere, J., Pliska, V. (1983) Hydrophobic parameters of amino acid side chains from partitioning of N-acetyl-amino-acid amides. *Eur. J. Med. Chem.* **18,** 369–375.
47. Mizrahi, A., Berdichevsky, Y., Ugolev, Y., Molshanski-Mor, S., Nakash, Y., Dahan, I., Alloul, N., Gorzalczany, Y., Sarfstein, R., Hirshberg, M., Pick, E. (2006) Assembly of the phagocyte NADPH oxidase complex: chimeric constructs derived from the cytosolic components as tools for exploring structure-function relationships. *J. Leukoc. Biol.* **79,** 881–895.
48. Macheroux, P., Kappes, B., Ealick, S. E. (2011) Flavogenomics—a genomic and structural view of flavin-dependent proteins. *FEBS J.* **278,** 2625–2634.
49. Chorev, M., Goodman, M. (1995) Recent developments in retro peptides and proteins—an ongoing topochemical exploration. *Trends Biotechnol.* **13,** 438–445.
50. Clark, R. A., Epperson, T. K., Valente, A. J. (2004) Mechanism of activation of NADPH oxidases. *Jpn. J. Infect. Dis.* **57,** S22–S23.
51. Kleinberg, M. E., Malech, H. L., Rotrosen, D. (1990) The phagocyte 47-kilodalton cytosolic oxidase protein is an early reactant in activation of the respiratory burst. *J. Biol. Chem.* **265,** 15577–15583.
52. Uhlinger, D. J., Tyagi, S. R., Lambeth, J. D. (1995) On the mechanism of inhibition of the neutrophil respiratory burst oxidase by a peptide from the C-terminus of the large subunit of cytochrome b_{558}. *Biochemistry* **34,** 524–527.
53. Katz, C., Levy-Beladev, L., Rotem-Bamberger, S., Rito, T., Rudiger, S. G. D., Friedler, A. (2011) Studying protein-protein interactions using peptide arrays. *Chem. Soc. Rev.* **40,** 2131–2145.
54. Rotrosen, D., Kleinberg, M. E., Nunoi, H., Leto, T., Gallin, J. L., Malech, H. L. (1990) Evidence for a functional cytoplasmic domain of phagocyte oxidase cytochrome b_{558}. *J. Biol. Chem.* **265,** 8745–8750.
55. Nakanishi, A., Imajoh-Ohmi, S., Fujinawa, T., Kikuchi, H., Kanegasaki, S. (1992) Direct evidence for interaction between COOH-terminal regions of cytochrome b_{558} subunits and cytsosolic 47-kDa protein during activation on $O_2\cdot^-$ generating system in neutrophils. *J. Biol. Chem.* **267,** 19072–19074.
56. Kleinberg, M. E., Mital, D., Rotrosen, D., Malech, H. L. (1992) Characterization of a phagocyte cytochrome b_{558} 91-kilodalton subunit functional domain: identification of peptide sequence and amino acids essential for activity. *Biochemistry* **31,** 2686–2690.
57. Tsuchiya, T., Imajoh-Ohmi, S., Nunoi, H., Kanegasaki, S. (1999) Uncompetitive inhibition of superoxide generation by a synthetic peptide corresponding to a predicted NADPH binding site in gp91^{phox}, a component of the phagocyte respiratory oxidase. *Biochem. Biophys. Res. Commun.* **257,** 124–128.
58. Koshkin, V., Pick, E. (1993) Generation of superoxide by purified and relipidated cytochrome b_{559} in the absence of cytosolic activators. *FEBS Lett.* **327,** 57–62.
59. Leusen, J. H. W., de Boer, M., Bolscher, B. G. J. M., Hilarius, P. M., Weening, R. S., Ochs, H. D., Roos, D., Verhoeven, A. J. (1994) A point mutation in gp91^{phox} of cytochrome b_{558} of the human NADPH oxidase leading to defective translocation of the cytosolic proteins p47^{phox} and p67^{phox}. *J. Clin. Invest.* **93,** 2120–2126.
60. Debeurme, F., Picciochi, A., Dagher, M-C., Grunwald, D., Beaumel, S., Fieschi, F., Stasia, M-J. (2010) Regulation of NADPH oxidase activity in phagocytes. Relationship between FAD/NADPH binding and oxidase complex assembly. *J. Biol. Chem.* **285,** 33197–33208.
61. Rae, J., Newburger, P. E., Dinauer, M. C., Noack, D., Hopkins, P. J., Kuruto, R., Curnutte, J. T. (1998) X-linked chronic granulomatous disease: mutations in the *CYBB* gene encoding the gp91^{phox} component of the respiratory-burst oxidase. *Am. J. Hum. Genet.* **62,** 1320–1331.
62. Heyworth, P. G., Cross, A. R., Curnutte, J. T. (2003) Chronic granulomatous disease. *Curr. Opin. Immunol.* **15,** 578–584.
63. Joseph, G., Gorzalczany, Y., Koshkin, V., Pick, E. (1994) Inhibition of NADPH oxidase activation by synthetic peptides mapping within the carboxy-terminal domain of small GTP-binding proteins. Lack of amino acid sequence specificity and importance of the polybasic motif. *J. Biol. Chem.* **269,** 29024–29031.
64. Hashida, S., Yuzawa, S., Suzuki, N. N., Fujioka, Y., Takikawa, T., Sumimoto, H., Inagaki, F., Fujii, H. (2004) Binding of FAD to cytochrome b_{558} is facilitated during activation of the phagocyte NADPH oxidase, leading to superoxide production. *J. Biol. Chem.* **279,** 26378–26386.

KEY WORDS:
superoxide · cytochrome b_{558} · p47^{phox} · p67^{phox} · Rac · amphiphile